ISSN 0915-633X

NATIONAL INSTITUTE FOR FUSION SCIENCE

Fast Wave Heating at Intermediate Ion Cyclotron Harmonics on the JIPP T-IIU Tokamak

Y. Takase, T. Watari, R. Kumazawa, T. Seki, K Adati, R. Ando,
T. Aoki, Y. Hamada, S. Hirokura, K. Ida, E. Kako, K. Kawahata,
Y. Kawasumi, K. Masai, K. Narihara, K. Ohkubo, M. Sakamoto,
F. Shimpo, Y. Taniguchi, K. Toi and T. Tsuzuki

(Received – Jan. 24, 1990)

NIFS-21 Feb. 1990

RESEARCH REPORT
NIFS Series

NAGOYA, JAPAN

FAST WAVE HEATING AT INTERMEDIATE ION CYCLOTRON HARMONICS ON THE JIPP T–II U TOKAMAK

Y. TAKASE,* T. WATARI, R. KUMAZAWA, T. SEKI,
K. ADATI, R. ANDO, T. AOKI, Y. HAMADA, S. HIROKURA,
K. IDA, E. KAKO, K. KAWAHATA, Y. KAWASUMI, K. MASAI,
K. NARIHARA, K. OHKUBO, M. SAKAMOTO, F. SHIMPO,
Y. TANIGUCHI, K. TOI, T. TSUZUKI
National Institute for Fusion Science,
Chikusa-ku, Nagoya,
Japan

ABSTRACT. Fast wave absorption and heating at a relatively high ion cyclotron harmonic ($\omega \simeq 6\Omega_D$) were studied on the JIPP T–II U tokamak. In spite of the low absorption efficiency predicted by a simple theory for present experimental parameters, appreciable electron and ion heating has been observed. Heating is most effective at relatively low densities $\overline{n}_e \simeq 1 \times 10^{19}\,\mathrm{m}^{-3}$. Ion tail was observed on the majority deuterium energy spectrum but not on the minority hydrogen spectrum, which suggests the possibility of direct absorption of mode-converted ion Bernstein wave power by deuterium ions. Because of the density rise caused by rf injection, a clear evidence of fast wave driven current was not observed.

Keywords: Fast Wave Current Drive, Fast Wave Heating, Density Limit, JIPP T–II U

* Massachusetts Institute of Technology, Cambridge, Massachusetts, U.S.A.

1. INTRODUCTION

Remarkable progress has been made in current drive by lower hybrid slow wave (LHSW) during the past decade [1,2]. Recently, a very efficient ($\eta_{CD} \equiv \bar{n}_e I_p R/P_{rf} \simeq 0.34 \times 10^{20}\,\mathrm{MA/MW\,m^{-2}}$) current drive by LHSW was demonstrated on the JT–60 tokamak [3]. Current drive by LHSW is currently the most reliable and most efficient method of noninductive current drive. However, LHSW which satisfy the accessibility condition damps by quasilinear electron Landau damping [4] near the plasma periphery in a reactor environment, and is not considered to be an efficient current driver in the plasma core. Fast wave at moderate to high harmonics of the ion cyclotron frequency (ICRF to LHRF) has favorable characteristics and is considered to be a promising method of current drive in hot, high density plasmas [5–9].

Fast wave current drive in a tokamak plasma was first reported by the JIPP T–II U group [10]. The experiment was performed in the lower hybrid range of frequencies (LHRF) at a frequency of 800 MHz in a low density slide-away regime. A current drive efficiency comparable to that of LHSW current drive was observed. However, no current drive was observed above the LHSW density limit. In a subsequent experiment on JIPP T–II U, plasma current was successfully started up with 40 MHz fast wave at a reduced toroidal field of $B_T = 0.2\,\mathrm{T}$ so that the wave frequency corresponded to $\omega = 13\Omega_H$ [11]. The plasma current was driven at a density 50 times higher than the lower hybrid density where $\omega = \omega_{LH}$. Recently an attempt was made to demonstrate fast wave current drive in a more standard tokamak plasma on the JFT–2 M tokamak [12]. Although electron heating was observed, no convincing evidence of fast wave current drive was observed. In contrast to the JFT–2 M experiment which operated at a relatively high harmonic ($\omega \gtrsim 10\Omega_H$) with low-field-side-launch antennas, the JIPP T–II U experiment operated at a relatively low harmonic ($\omega \simeq 3\Omega_H = 6\Omega_D$) and used high-field-side-launch antennas (the same antennas as those used for the previous 40 MHz ICRF experiments).

In the present paper, results from the fast wave experiments performed on the JIPP T–II U tokamak are reported. In Sec. 2 the experimental setup is described. Efficiencies of wave absorption by electrons and mode conversion are estimated based on present theoretical knowledge in Sec. 3. Results from heating and absorption experiments are reported in Sec. 4. Attempts to drive plasma current with 130 MHz waves are described in Sec. 5. Finally, conclusions are given in Sec. 6.

2. EXPERIMENTAL SETUP

JIPP T–II U tokamak was run with parameters $R = 0.91\,\mathrm{m}$, $a = 0.23\,\mathrm{m}$, $B_T = 3\,\mathrm{T}$, and $I_p = 220\,\mathrm{kA}$. Two rf systems with frequencies 130 MHz and 40 MHz were used. Four high-field-side-launch antennas located on adjacent ports, as shown in Fig. 1, were used to launch up to 400 kW of 130 MHz rf power (the rf power is defined as the power radiated from the antenna, i.e., incident power minus reflected power minus circuit loss). The phasing of the four-element antenna array was usually set to $\Delta\phi = 180°$ to maximize $n_\parallel$, and therefore to maximize the chance of absorption. At a toroidal field of 3 T, 130 MHz corresponds to $\omega \simeq 3\Omega_H = 6\Omega_D$. The lower hybrid layer corresponds to a density of $n_e \simeq 8 \times 10^{17}\,\mathrm{m}^{-3}$, and is located in the shadow of the limiter so that LHSW cannot play any role. Initial 130 MHz fast wave experiments on JIPP T–II U concentrated on the absorption characteristics of the fast wave in such a frequency regime. Two high-field-side-launch antennas located on adjacent ports with power handling capabilities of about 400 kW each were used to inject rf power at 40 MHz. Electron heating in the ion-ion hybrid regime (or mode-conversion regime) on JIPP T–II U using the 40 MHz system has been documented in previous publications [13–15]. The 40 MHz system was used in the present experiments for comparison purposes.

Prior to these experiments, the wall of the tokamak was carbonised by running a glow discharge in a mixture of CH_4 and H_2. Titanium gettering was used throughout the present experiment in an effort to minimize the density rise during rf injection. Most of the experiments were performed in deuterium majority plasmas with hydrogen minority concentrations of typically $n_H/(n_D + n_H) = 10\text{–}30\%$, which corresponds to the ion-ion hybrid regime for the 40 MHz system. The hydrogen concentration was controlled by using a filling gas and gas puffing of 100% deuterium, 90% deuterium + 10% hydrogen, or 100% hydrogen, and was measured by a mass-resolving charge exchange neutral analyzer.

3. THEORETICAL ESTIMATES

Ray tracing calculations for the fast wave under JIPP T–II U experimental conditions were performed using a modified version of the Bonoli ray tracing code [16]. The result showed that because the fast wave is excited from the high-field side, $n_{\|}$ mainly downshifts due to the $1/R$ effect. The projection of a ray trajectory on a poloidal cross section and the variation of $n_{\|}$ along the ray trajectory are shown in Figs. 2(a) and (b). Mode-conversion effects are not included in the calculation. Since no significant upshifts of $n_{\|}$ is predicted from a purely toroidal effect, direct absorption of fast wave power by electrons is expected to be inefficient for JIPP T–II U parameters unless $n_{\|}$ is upshifted due to other mechanisms such as scattering from density fluctuations [7]. Parametric decay is not considered to play an important role because no significant parametric decay activity was detected by either the electrostatic or the electromagnetic probe. The spatial power damping rate given in Ref. [9] is calculated to be $2k_{\perp Im} < 10^{-4}\,\mathrm{cm}^{-1}$ for parameters of the present experiment.

The fraction of mode converted power may be estimated by evaluating the tunneling parameter η, which is defined by the relationship $|T|^2 = \exp(-\eta)$ where T is the transmission coefficient. According to a recently proposed formula [17] applicable to mode conversion at high ion cyclotron harmonics in a single species plasma, η is insignificantly small (10^{-3} at most for $\omega = 3\Omega_H$ in a hydrogen plasma, much smaller for $\omega = 6\Omega_D$ in a deuterium plasma), and therefore mode conversion is not predicted to be important. However, there is still a possibility that mode conversion may play a more significant role in a multiple ion species plasma, or when single-pass absorption is weak and multiple passes across the mode conversion layer must be considered.

4. WAVE ABSORPTION AND HEATING RESULTS

Initial comparison of the 130 MHz system with the 40 MHz system was made with unconditioned walls and antennas in a deuterium plasma with approximately 20% hydrogen minority concentration. Effects on the plasma were comparable, with a small difference in the loop voltage response. A large density increase was observed when rf power was injected from either the 130 MHz or the 40 MHz system. Electron heating was nearly identical. As conditioning of the antennas and the limiter/wall proceeded, however, the density rise caused by the injection of 40 MHz power decreased and the electron heating increased. On the other hand, the density rise caused by the injection of 130 MHz power remained large. Although the central electron temperature obtained with the 40 MHz system is higher, the stored energy (evaluated at the same density) is nearly the same.

Figure 3 displays typical effects of 130 MHz waves (the first rf pulse) and 40 MHz waves (the second rf pulse) on a deuterium majority plasma with a hydrogen minority concentration of approximately 30%. The toroidal magnetic field was $B_T = 3\,\mathrm{T}$, and the plasma current was $I_p = 220\,\mathrm{kA}$. The phasing of the 130 MHz antennas was set to $\Delta\phi = 180°$. The 40 MHz power was injected from only one antenna. The plasma response to the 130 MHz waves under such a condition is described below.

The density increase caused by injection of 130 MHz rf power was significantly greater than that caused by injection of 40 MHz power. Such a difference is expected because of lower single-pass absorption efficiency and consequently higher rf fields in the plasma edge region predicted for 130 MHz, which can result in increased plasma-wall interactions.

The central electron temperature [Fig. 3(e)], measured by electron cyclotron emission calibrated by soft X-ray pulse height analysis, increases by 300 eV from an initial temperature of 1300 eV at a target density of $\overline{n}_e \simeq 1 \times 10^{19}\,\mathrm{m}^{-3}$. The electron temperature starts rising immediately on rf turn-on, indicating direct absorption of the launched wave by electrons. The ion temperature, measured by charge exchange neutral analysis, increases from 300 eV to 800 eV. However, both electron and ion temperatures decrease subsequently because of the density rise. If a similar density rise were reproduced by gas puffing alone, the electron temperature would drop immediately with the density increase.

Shrinking of the electron temperature profile (as measured by a 10-channel ECE system) and the current density profile (as inferred from the internal inductance ℓ_i) are observed. A positive spike on the loop voltage is observed at rf turn-on [Figs. 3(b) and (c)], whose magnitude is consistent with the observed change of internal inductance. The time scale ($\simeq$ 10 ms) for the voltage spike suggests that the current density profile change occurred near the plasma surface. Broadening of the electron temperature and current density profiles are observed at rf turn-off. The apparent delay in the recovery of the loop voltage is caused by the decreasing internal inductance.

Charge exchange neutral spectra obtained over several shots identical to the one shown in Fig. 3 are displayed in Fig. 4. During the injection of 40 MHz power a high energy component is formed on the hydrogen flux, which is consistent with some fraction of power being absorbed directly by the minority hydrogen ions at its fundamental resonance. Under the present experimental condition, the fraction of 40 MHz rf power absorbed by the minority hydrogen is theoretically expected to be in the range of 1–10% according to a slab geometry full-wave calculation [18]. In contrast, no high energy hydrogen flux is observed during the injection of 130 MHz power. Instead, a high energy component is observed on deuterium ions. This somewhat unexpected behaviour points to the possibility of direct absorption of mode-converted ion Bernstein waves by deuterium. For hydrogen ions the only ion-cyclotron harmonic resonance is $\omega = 3\Omega_H$ located at $R \simeq 0.96\,\mathrm{m}$. For deuterium ions $\omega = 6\Omega_D$ ($R \simeq 0.96\,\mathrm{m}$) and $\omega = 5\Omega_D$ ($R \simeq 0.80\,\mathrm{m}$) resonances exist in the plasma interior, and the $\omega = 7\Omega_D$ resonance exists at the plasma edge ($R \simeq 1.12\,\mathrm{m}$). A most plausible scenario would be mode conversion of fast wave to IBW at $\omega = 6\Omega_D$ ($R \simeq 0.96\,\mathrm{m}$) and subsequent absorption of the mode-converted IBW by deuterium ions at $\omega = 5\Omega_D$ ($R \simeq 0.80\,\mathrm{m}$). Although the fraction of rf power absorbed directly by ions cannot be determined accurately from the available data, a much higher mode conversion efficiency than what is predicted by a simple theory [17] may be required to explain this result.

Most noticeable heating was observed at relatively low densities $\overline{n}_e \simeq (1\text{–}2)\times 10^{19}\,\mathrm{m}^{-3}$. Heating becomes less effective at higher densities. The central electron temperature just before and just after rf turn-on, and just before and just after rf turn-off are shown as a function of density in Fig. 5. Because density is increasing at rf turn-on but is decreasing at rf turn-off, the effect of changing density must be taken into account in order to assess the effectiveness of rf heating. The change in central electron energy density at rf turn-on Δw_{e0}^{on} and at rf turn-off Δw_{e0}^{off}, where $w_{e0} \equiv \frac{3}{2} n_{e0} T_{e0}$, normalized by the volume averaged rf energy input $\langle w_{rf} \rangle \equiv P_{rf} \Delta t / V$, are shown as functions of density in Fig. 6. The diamagnetically determined stored energy of the ohmic and rf-heated plasmas are shown as a function of density in Fig. 7. The stored energy is evaluated when $\dot{W} = 0$. The injected rf power was deliberately lowered for the two low density rf shots in order to limit the density rise. The points shown by open squares indicate the values of stored energy expected to be obtained at the same power level as for higher density shots, assuming that the incremental stored energy is proportional to the incremental heating power (offset linear power scaling).

The absorbed rf power can be estimated from the change in time derivative of the stored energy at rf turn-on and rf turn-off. The "absorption efficiency", defined as

$P_{abs}/P_{rf} \equiv \Delta\dot{W}/P_{rf}$, is in the range 40–80% in the range of density studied, and decreases with density as shown in Fig. 8. For the particular case shown in Fig. 3, the central absorbed rf power density is $\dot{w}_0 = 0.90\,\mathrm{MW/m^{-3}}$, which consists of $\frac{3}{2}\dot{n}_{e0}T_{e0} = 0.38\,\mathrm{MW/m^{-3}}$, $\frac{3}{2}n_{e0}\dot{T}_{e0} = 0.24\,\mathrm{MW/m^{-3}}$, $\frac{3}{2}\dot{n}_{i0}T_{i0} = 0.07\,\mathrm{MW/m^{-3}}$, and $\frac{3}{2}n_{i0}\dot{T}_{i0} = 0.21\,\mathrm{MW/m^{-3}}$, where the dot represents the time derivative. Since the volume-averaged absorbed rf power density is $\langle\dot{w}\rangle = 0.24\,\mathrm{MW/m^{-3}}$, the peaking factor is $\dot{w}_0/\langle\dot{w}\rangle \simeq 4$.

Heating with the 130 MHz system becomes slightly less effective when the phasing is changed to $\Delta\phi = 90°$ or when a hydrogen majority plasma is used instead of a deuterium majority plasma, but the difference is small. In contrast, heating with the 40 MHz system in a hydrogen majority plasma, in which efficient absorption is not expected, is much less efficient than in a deuterium majority plasma (and is less efficient than with the 130 MHz in a hydrogen plasma).

5. CURRENT DRIVE RESULTS

Attempt was made to increase electron absorption by combining lower hybrid current drive (LHCD) and 130 MHz ICRF heating. Although increase is observed on electron cyclotron emission initially, indicating direct coupling of the wave power to electrons, the density rise caused by injection of the 130 MHz power slowed down the superthermal electrons produced by LHCD, and successful results were not obtained.

Start-up of the plasma current by fast wave alone was also tried. Only steady state toroidal field and steady state vertical field were applied. The present experiment was performed mostly at a toroidal field of $B_T = 0.46\,\mathrm{T}$ in a deuterium majority plasma, which corresponds to $\omega \simeq 11\Omega_D$ for 40 MHz and $\omega \simeq 37\Omega_D$ for 130 MHz, with a vertical field of 10 G. As reported previously [11], it was possible to drive plasma current with the 40 MHz system, but only at low filling pressures ($p \lesssim 3 \times 10^{-4}$ Torr). While it was possible to create a currentless low density ($\overline{n}_e \lesssim 2 \times 10^{18}\,\mathrm{m^{-3}}$) plasma with 130 MHz power alone, the range of filling pressures for successful plasma creation was restricted to higher pressures ($p \gtrsim 3 \times 10^{-4}$ Torr), and the amount of rf current driven by the 130 MHz system was much less than 1 kA. A more careful parameter search (toroidal field, vertical field, rf power, filling pressure) is required to find an optimum condition. In particular, a higher toroidal field and a correspondingly higher vertical field may be required for 130 MHz, which was beyond the capability of the vertical field power supply used in these experiments.

6. CONCLUSIONS

In conclusion, electron and ion heating by 130 MHz ICRF fast wave at a relatively high harmonic of ion cyclotron frequency ($\omega \simeq 6\Omega_D = 3\Omega_H$) has been observed. Despite the low absorption efficiency predicted by theory, the heating efficiency is comparable to that obtained with the 40 MHz fast wave. The absorption efficiency, as inferred from the change in time derivative of the stored energy at rf turn-on and turn-off, was typically over 50%. Heating is most effective at low density, but unlike with 40 MHz, heating is insensitive to the concentration ratio of hydrogen to deuterium. The density rise is larger with the 130 MHz system except with unconditioned antenna and/or limiter/wall, which may be attributed to its lower single-pass absorption. Direct electron heating was inferred from the time response of the electron temperature at rf turn-on and turn-off. Ion tail was observed on the deuterium energy spectrum, which suggests the possibility of direct absorption of mode-converted IBW power by deuterium ions. These results suggest that a very low (1% or less) single-pass absorption may be acceptable if surface interactions could be controlled, and that multiple-pass effects are very important.

Current drive by 130 MHz ICRF fast wave was not successfully demonstrated. A more effective control of the density rise by more careful conditioning of the antennas, limiters, and walls will be necessary in order to demonstrate a convincing evidence of fast wave current drive.

ACKNOWLEDGMENTS

This experiment was performed while one of the authors (Y. T.) was visiting NIFS under the US-Japan personnel exchange program. He would like to thank the members of the JIPP T–II U Group for their hospitality and cooperation during his stay, Dr. P. Bonoli for the use of his ray tracing code, and Drs. K. Itoh, S.-I. Itoh, and M. Porkolab for useful discussions. He was supported by the US Department of Energy Contract No. DE–AC02–78ET51013. NIFS is supported by the Japanese Ministry of Education.

REFERENCES

[1] For review of LHCD theory, see: FISCH, N. J., Rev. Mod. Phys. **59** (1987) 175.

[2] For review of LHCD experiments, see for example: HOOKE, W., Plasma Phys. and Controlled Fusion **26** (1984) 133; PORKOLAB, M., in Wave Heating and Current Drive in Plasmas, edited by GRANASTEIN, V. L., COLESTOCK, P. L. (Gordon and Breach, New York, 1985), p. 219.

[3] UEHARA, K., KIMURA, H., JT–60 TEAM, in Radio-Frequency Power in Plasmas (Proc. 8th Topical Conf. Irvine, 1989), AIP, New York (1989) 106.

[4] BRAMBILLA, M., in Physics of Plasmas Close to Thermonuclear Conditions (Proc. Int. School of Plasma Physics Varenna, 1979), Vol. 1, CEC, Brussels (1980) 291.

[5] WONG, K.-L., ONO, M., Nucl. Fusion **23** (1983) 805.

[6] EHST, D. A., in Non-Inductive Current Drive in Tokamaks (Proc. IAEA Technical Committee Meeting Culham, 1983), Vol. 2 (1983) 442.

[7] ANDREWS, P. L., BHADRA, D. K., Nucl. Fusion **26** (1986) 897.

[8] EHST, D. A., Argonne National Laboratory Report ANL/FPP/TM–219, 1988.

[9] CHIU, S. C., CHAN, V. S., HARVEY, R. W., PORKOLAB, M., General Atomics Report GA–A19534, submitted to Nucl. Fusion.

[10] OHKUBO, K., HAMADA, Y., OGAWA, Y., et al., Phys. Rev. Lett. **56** (1986) 2040.

[11] ANDO, R., KAKO, E., OGAWA, Y., WATARI, T., Nucl. Fusion **26** (1986) 1619.

[12] YAMAMOTO, T., UESUGI, Y., KAWASHIMA, H., et al., Phys. Rev. Lett. **63** (1989) 1148.

[13] WATARI, T., OHKUBO, K., AKIYAMA, R., et al., in Plasma Physics and Controlled Nuclear Fusion Research 1986 (Proc. 11th Int. Conf. Kyoto, 1986), Vol. 1, IAEA, Vienna (1987) 495.

[14] IDA, K., OGAWA, Y., WATARI, T., et al., in Controlled Fusion and Plasma Physics

(Proc. 14th Europ. Conf. Madrid, 1987), Part III, European Physical Society (1987) 870.

[15] ANDO, R., SATO. K., WATARI, T., et al., Nucl. Fusion **28** (1988) 577.

[16] BONOLI, P. T., ENGLADE, R. C., Phys. Fluids **29** (1986) 2937.

[17] CHIU, S. C., CHAN, V. S., HARVEY, R. W., PORKOLAB, M., in Radio-Frequency Power in Plasmas (Proc. 8th Topical Conf. Irvine, 1989), AIP, New York (1989) 230.

[18] BRAMBILLA, M., Nucl. Fusion **28** (1988) 549.

FIGURE CAPTIONS

FIG. 1. A plan view of the JIPP T–II U tokamak. Locations of the antennas are shown.

FIG. 2. (a) The projection of fast wave rays on a poloidal cross section. (b) The variation of $n_{\|}$ along the ray trajectory. Deuterium plasma, 130 MHz, $B_T = 3\,\mathrm{T}$, $I_p = 220\,\mathrm{kA}$, $\overline{n}_e = 2 \times 10^{19}\,\mathrm{m}^{-3}$, $n_{\|0} = 5$. The horizontal axis is the toroidal angle ϕ along the ray trajectory.

FIG. 3. Typical effects of 130 MHz waves (the first rf pulse) and 40 MHz waves (the second rf pulse). Deuterium majority plasma, 30% hydrogen minority, $B_T = 3\,\mathrm{T}$, $I_p = 220\,\mathrm{kA}$, $P_{130\,\mathrm{MHz}} = 220\,\mathrm{kW}$, $P_{40\,\mathrm{MHz}} = 250\,\mathrm{kW}$, $\Delta\phi_{130\,\mathrm{MHz}} = 180°$. Only one antenna was used for 40 MHz. (a) I_p (kA); (b) V_l (V); (c) P_{OH}, $P_{130\,\mathrm{MHz}}$, $P_{40\,\mathrm{MHz}}$ (MW); (d) $\overline{n}_e$ ($10^{19}\,\mathrm{m}^{-3}$); (e) T_{e0}^{ECE} (keV); (f) W_{dia}, W_{equ} (kJ). W_{equ} is the smoother curve in (f) and a constant ℓ_i of 1.35 was assumed.

FIG. 4. Hydrogen and deuterium charge exchange neutral spectra at different times. (a) H, OH; (b) H, 130 MHz; (c) H, 40 MHz; (d) D, OH; (e) D, 130 MHz; (f) D, 40 MHz. Same parameters as Fig. 3.

FIG. 5. The central electron temperature measured by ECE just before (open circle) and just after (solid circle) rf turn-on, and just before (solid square) and just after (open square) rf turn-off as a function of density. D(H), $B_T = 3\,\mathrm{T}$, $I_p = 220\,\mathrm{kA}$, $300 \leq P_{130\,\mathrm{MHz}} \leq 400\,\mathrm{kW}$, $\Delta\phi_{130\,\mathrm{MHz}} = 180°$.

FIG. 6. The change in central electron energy density $w_{e0} \equiv \frac{3}{2} n_{e0} T_{e0}$ at rf turn-on Δw_{e0}^{on} (solid circles) and rf turn off Δw_{e0}^{off} (open circles), normalized by volume averaged rf energy input $\langle w_{\mathrm{rf}} \rangle \equiv P_{\mathrm{rf}} \Delta t / V$, as a function of density.

FIG. 7. The diamagnetically determined stored energy of the ohmic (solid circles) and rf-heated plasmas (open triangles) as a function of density. The rf power was lower for the two low density shots. The open squares indicate expected stored energies at the same

power level as for higher density shots.

FIG. 8. The "absorption efficiency" $\Delta\dot{W}/P_{\rm rf}$ determined at rf turn-on (solid circles) and rf turn-off (open circles) as a function of density.

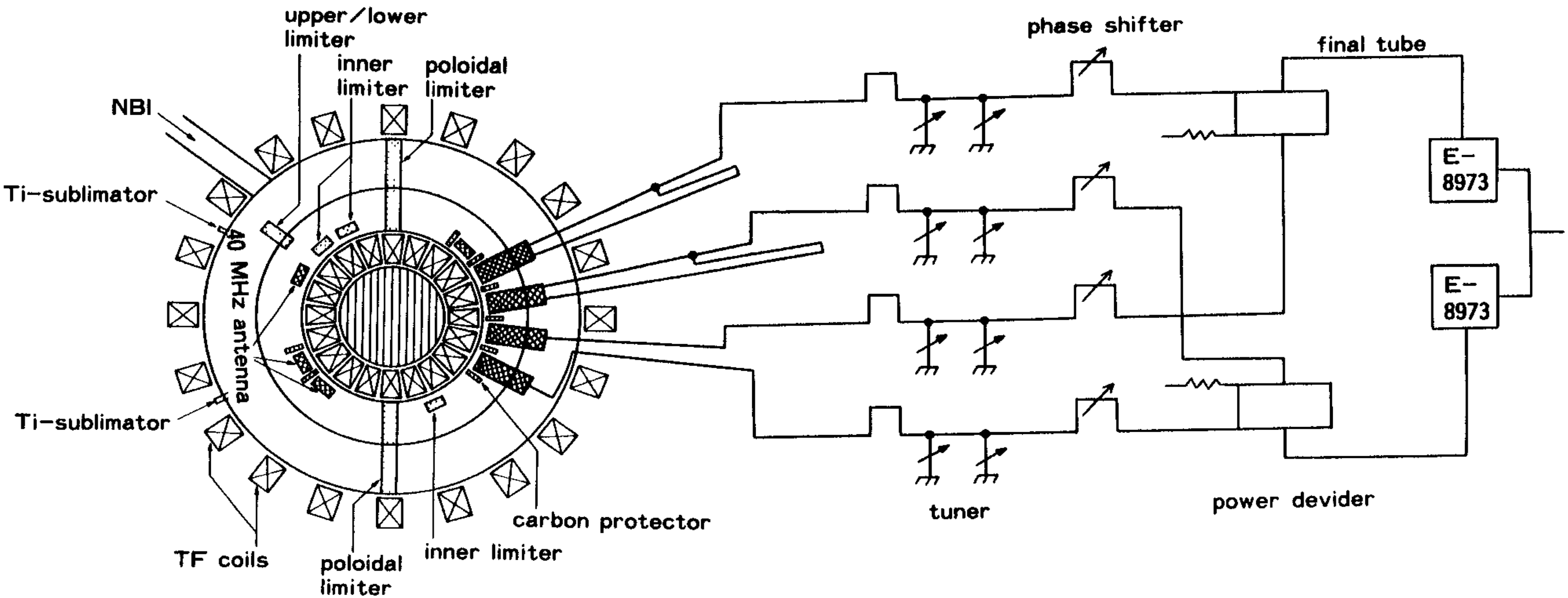

JIPP T-II U 130MHz RF System

FIG. 1.

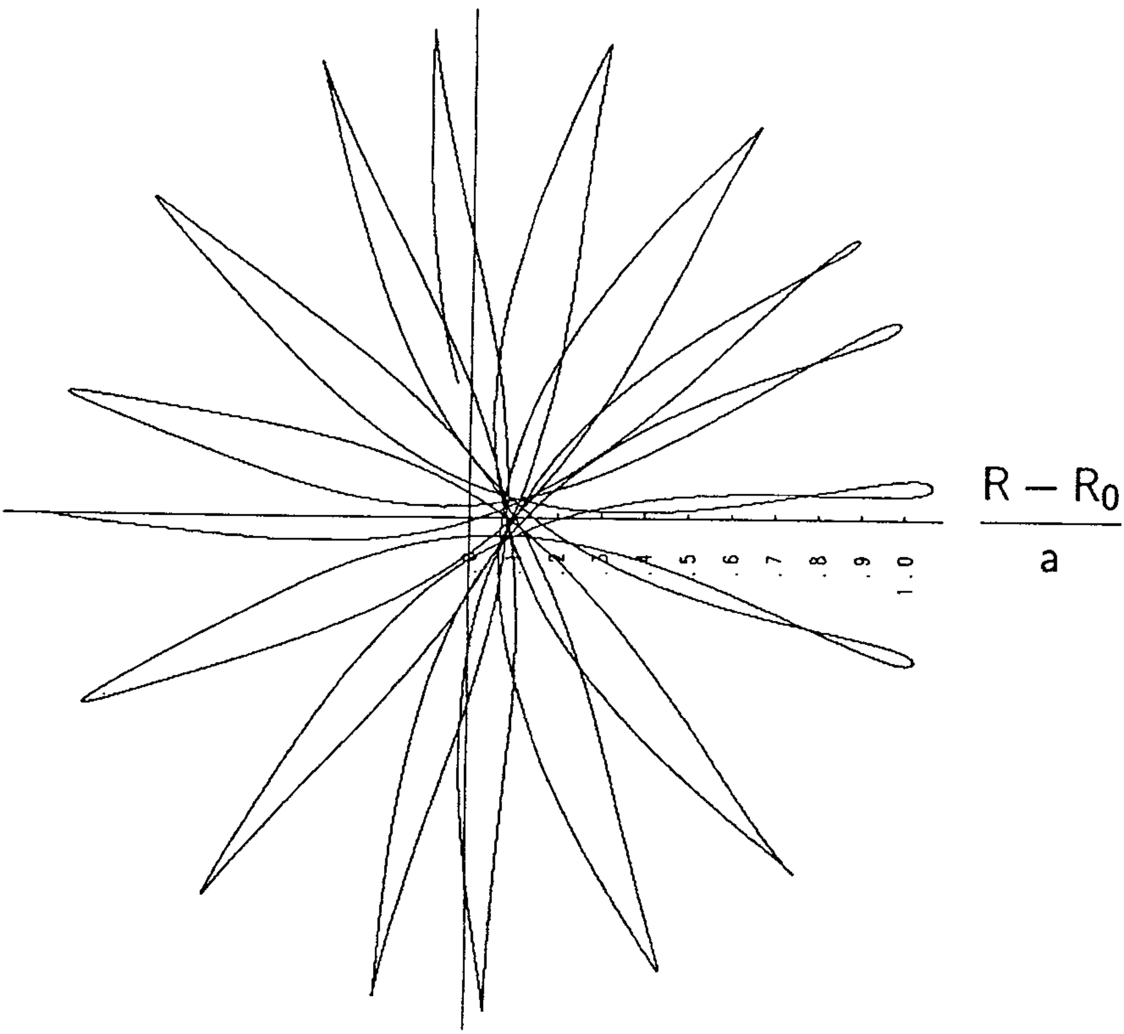

FIG. 2(a)

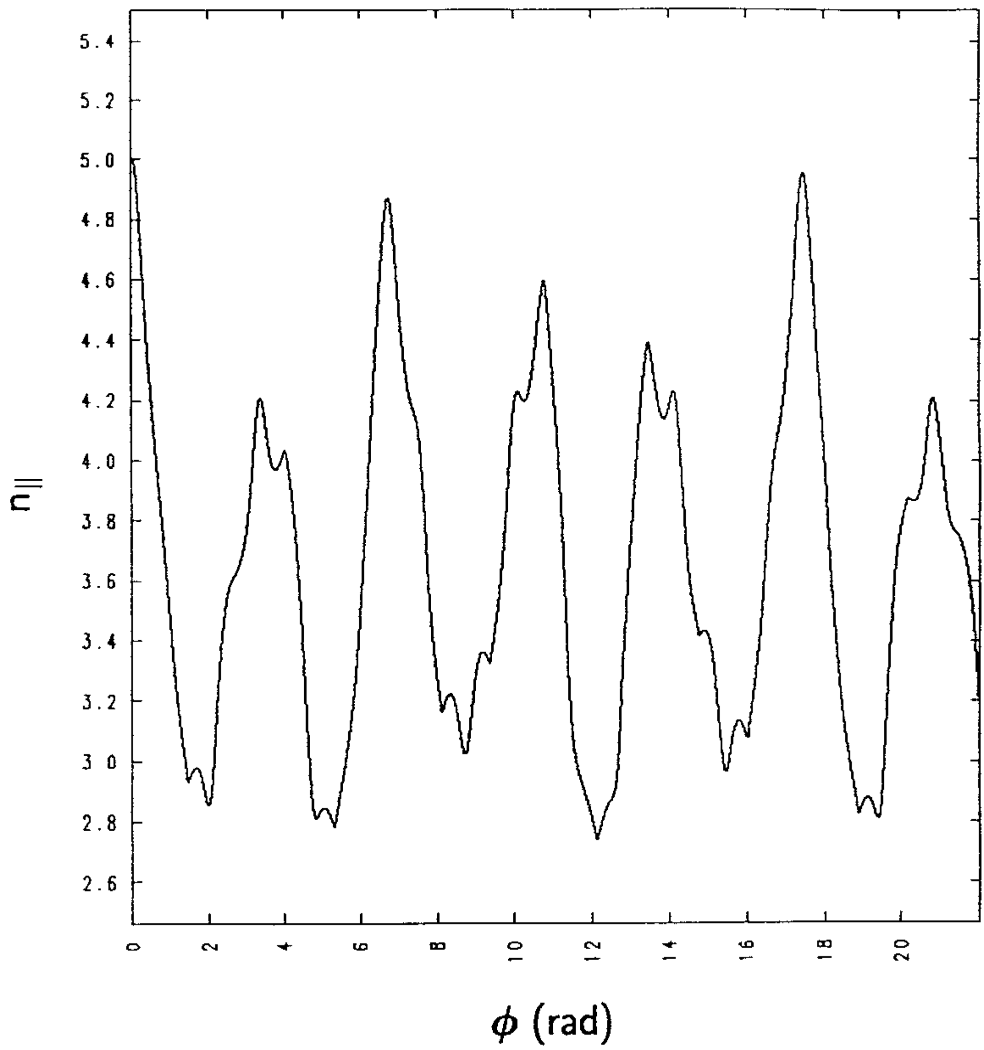
5.4
5.2
5.0
4.8
4.6
4.4
4.2
4.0
3.8
3.6
3.4
3.2
3.0
2.8
2.6
$n_{||}$
0
2
4
6
8
10
12
14
16
18
20
ϕ (rad)

FIG. 2(b)

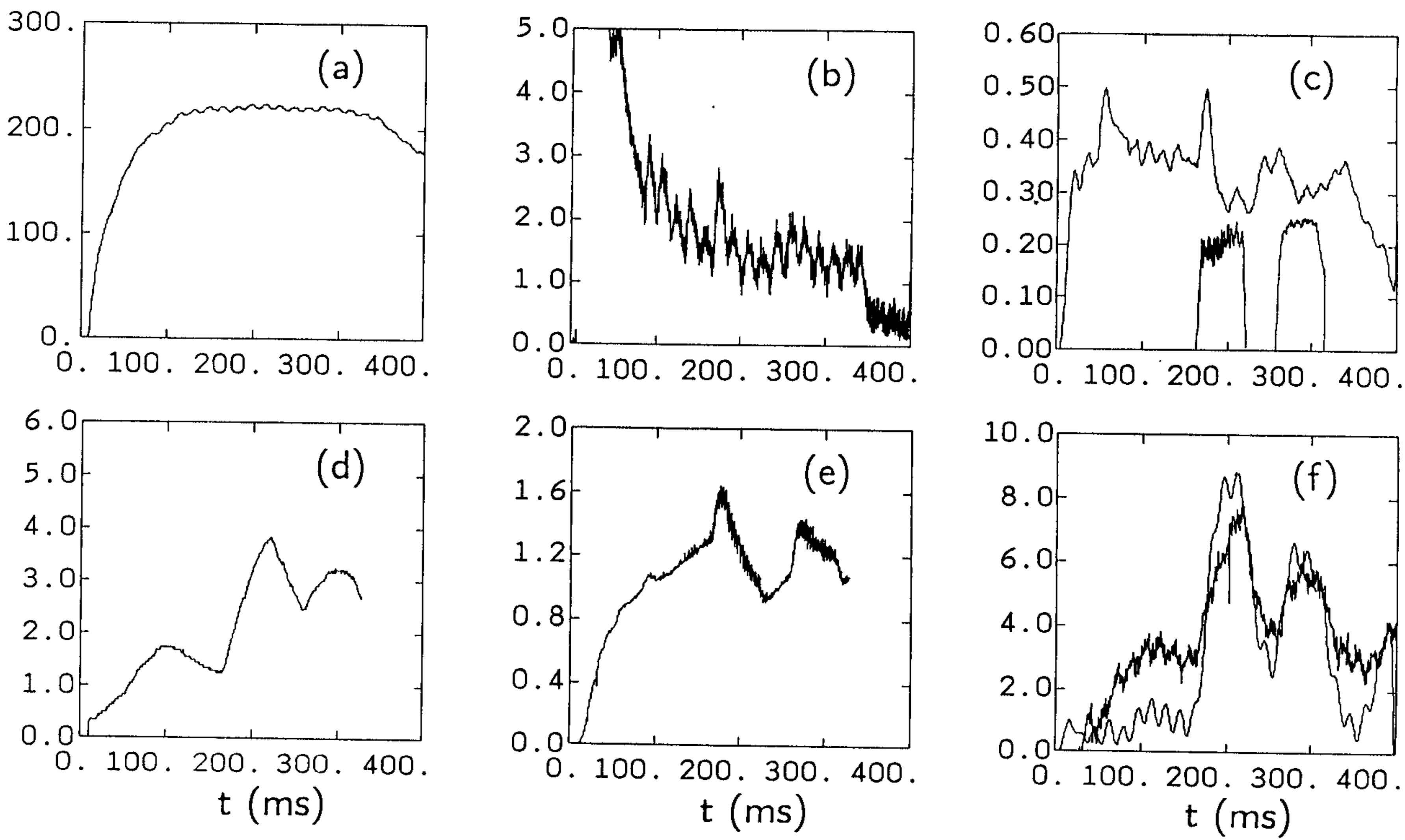

FIG. 3

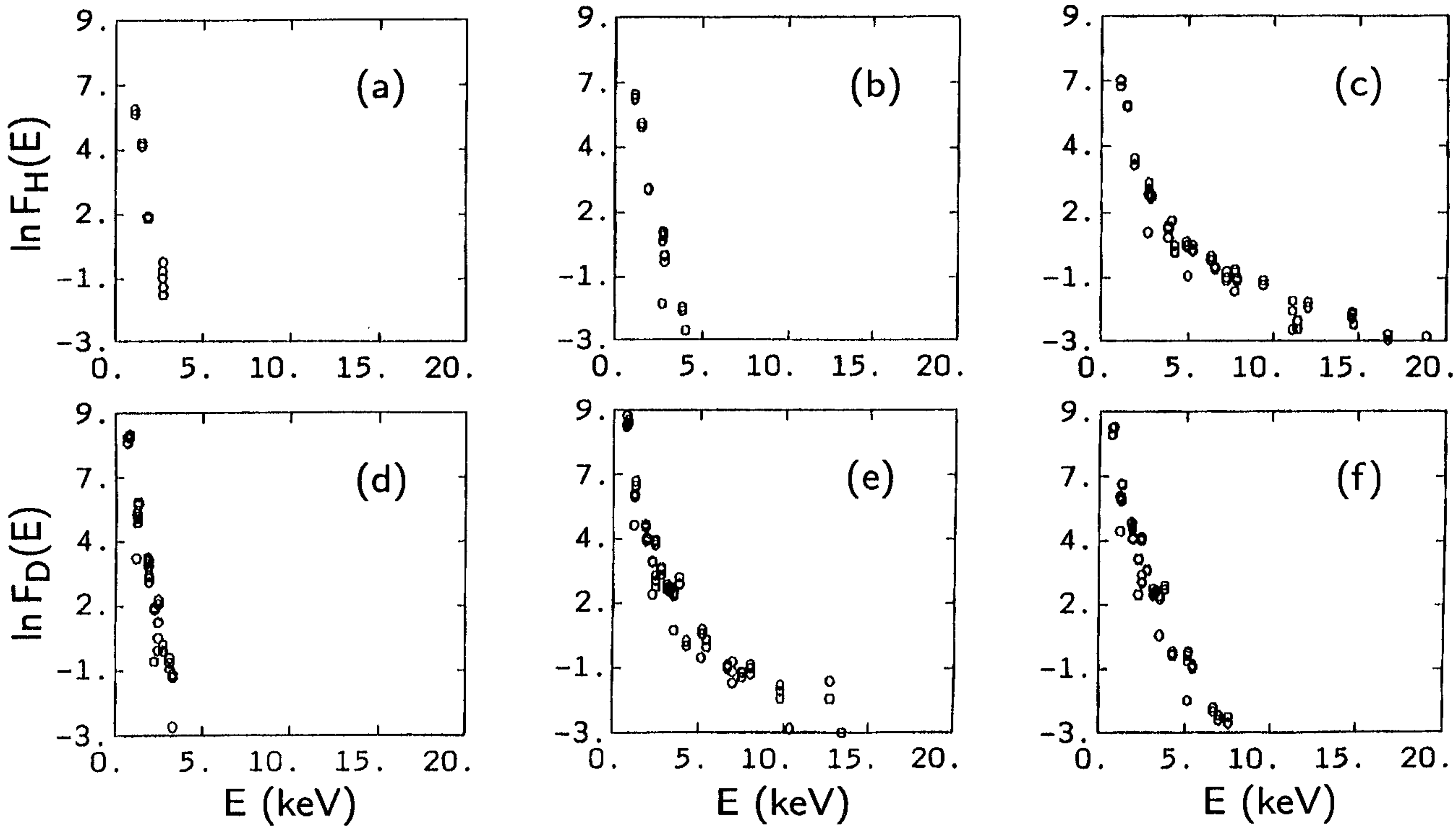

FIG. 4

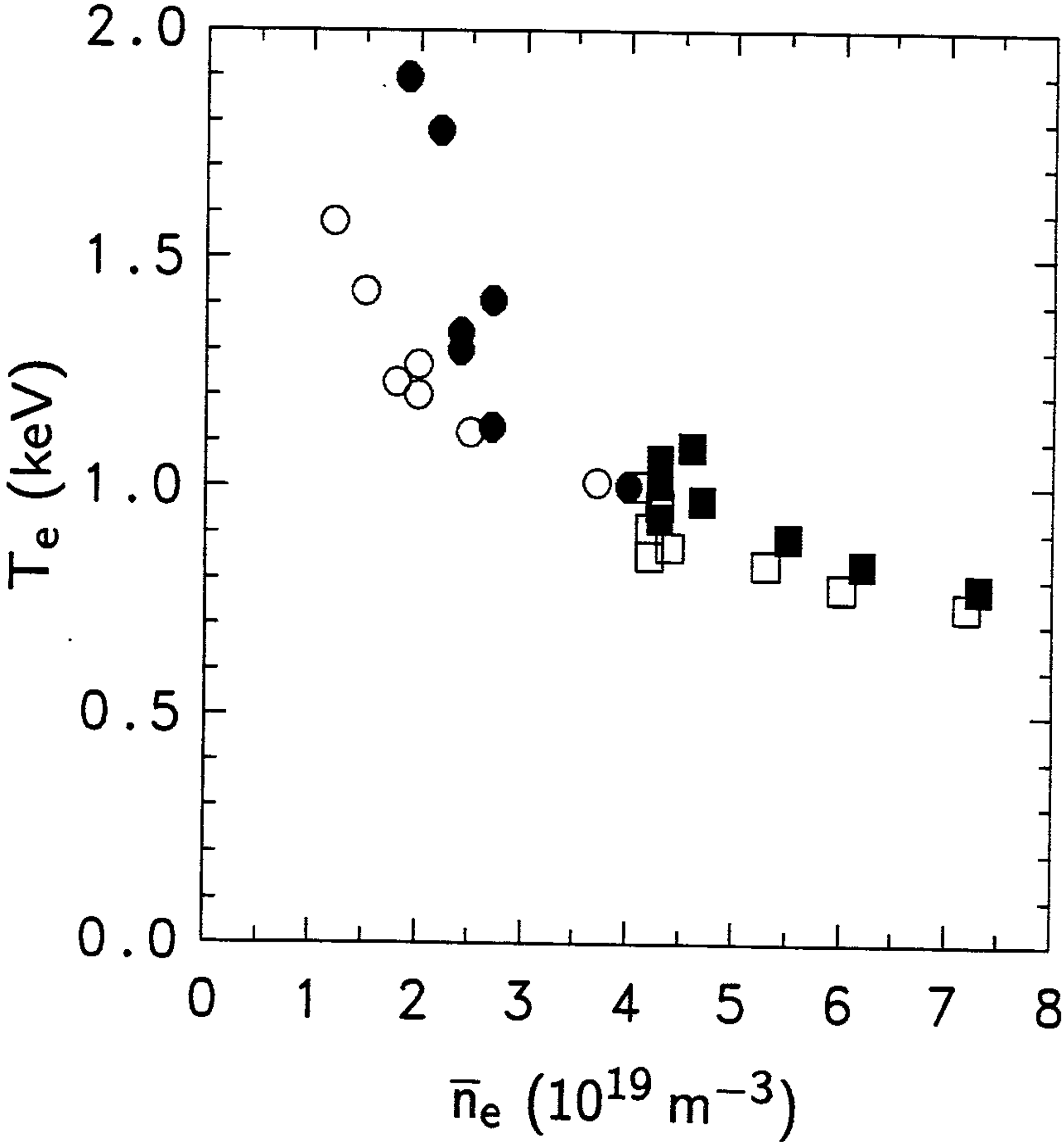

FIG. 5

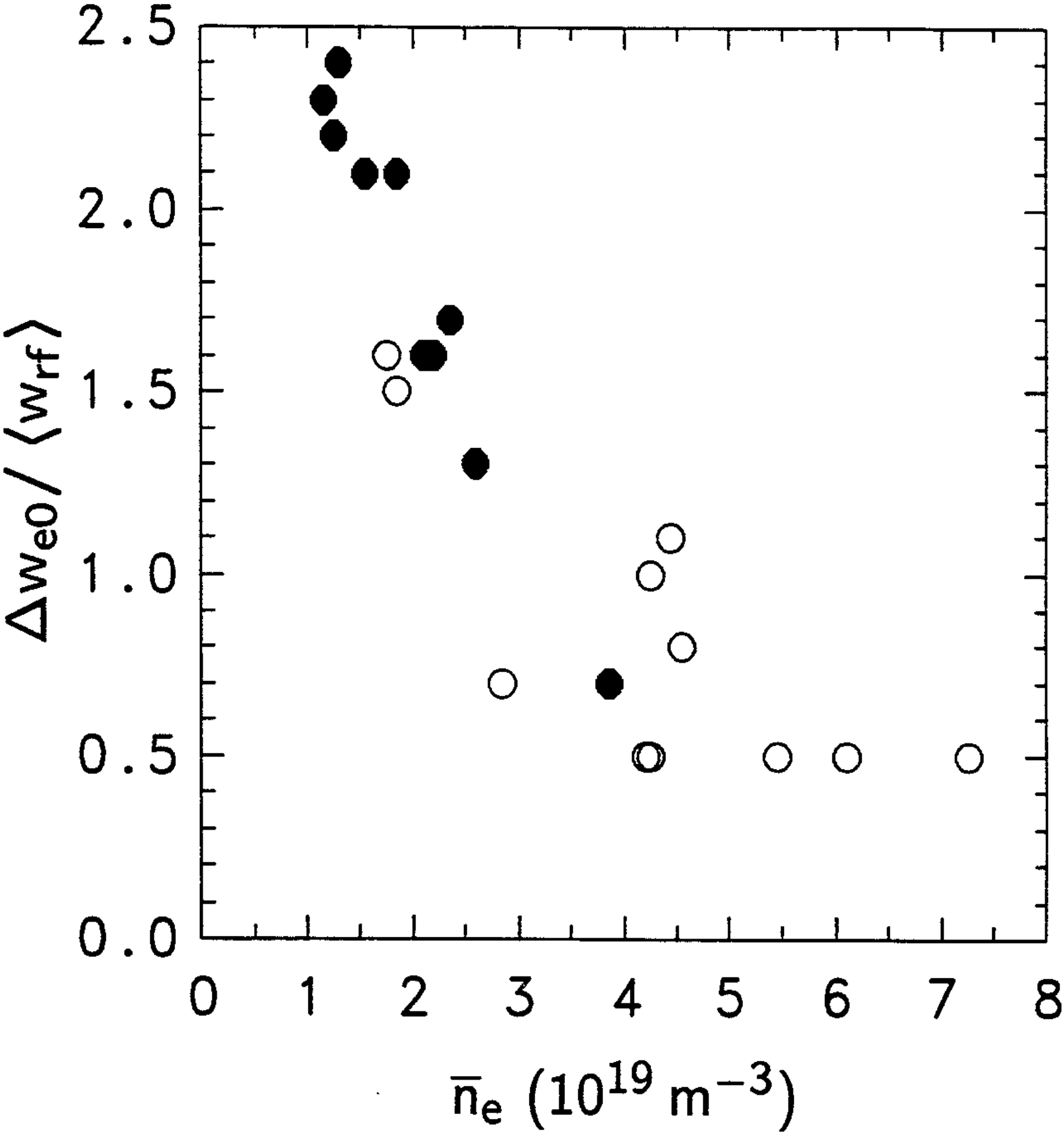

FIG. 6

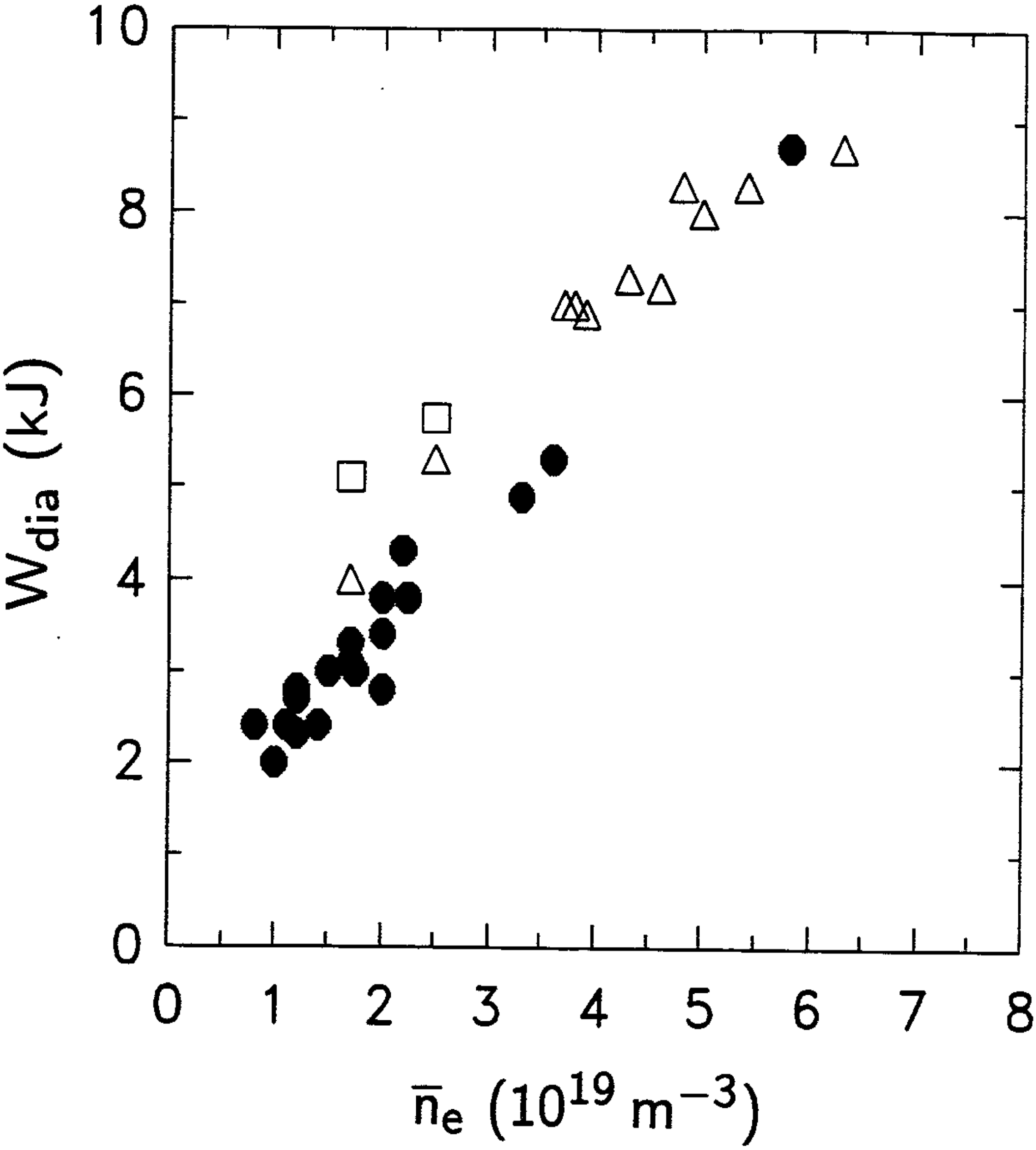

FIG. 7

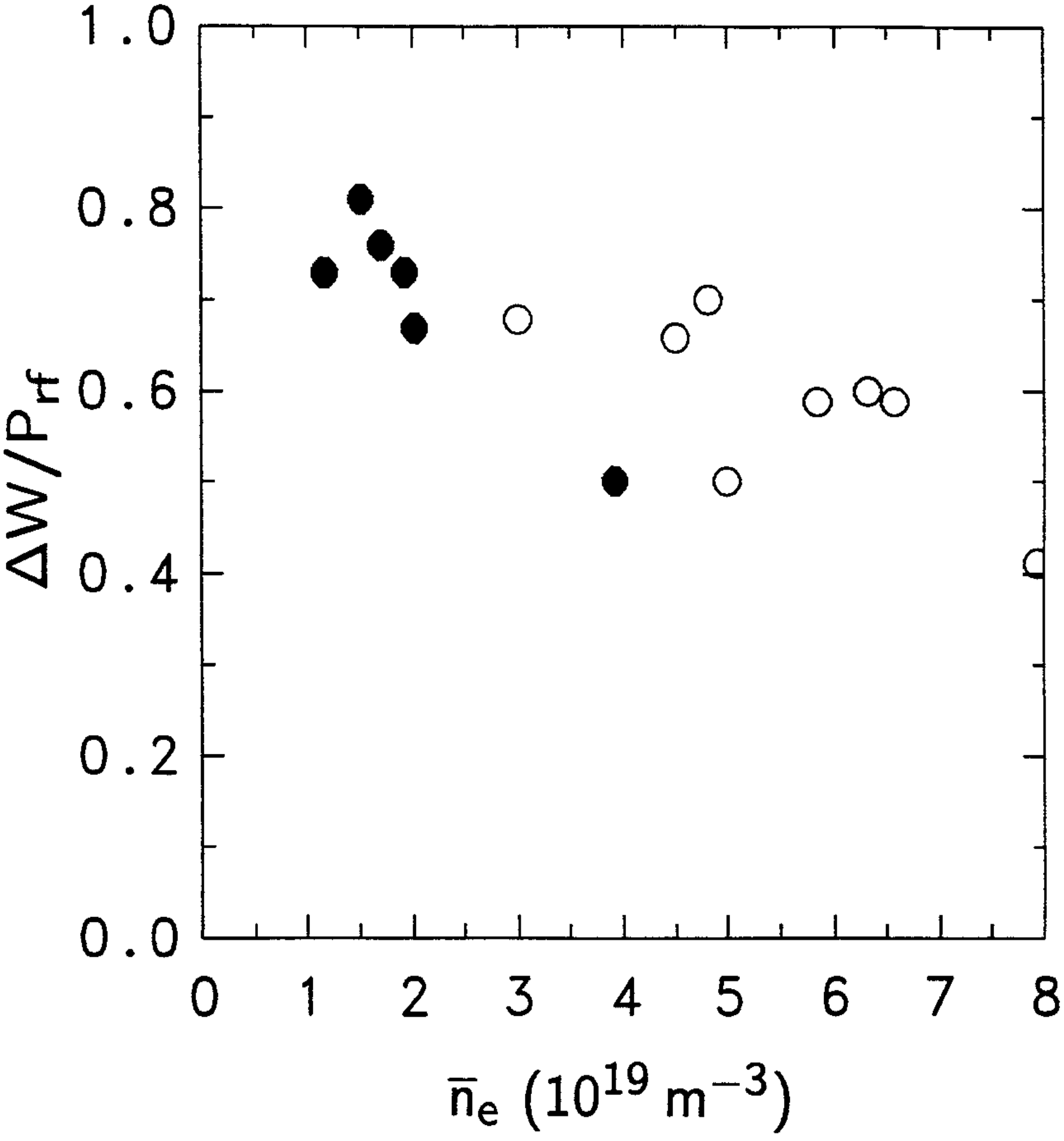

FIG. 8